Title	Darkening effect on AZ31B magnesium alloy surface induced by nanosecond pulse Nd:YAG laser
Author(s)	Guan, Y.C.; Zhou, W.; Zheng, H.Y.; Li, Z.L.
Citation	Guan, Y., Zhou, W., Zheng, H.,& Li, Z. (2013). Darkening effect on AZ31B magnesium alloy surface induced by nanosecond pulse Nd:YAG laser. Applied Surface Science, 280, 462-466.
Date	2013
URL	http://hdl.handle.net/10220/39986
Rights	© 2013 Published by Elsevier B.V. This is the author created version of a work that has been peer reviewed and accepted for publication by Applied Surface Science, Elsevier. It incorporates referee's comments but changes resulting from the publishing process, such as copyediting, structural formatting, may not be reflected in this document. The published version is available at: [http://dx.doi.org/10.1016/j.apsusc.2013.05.011].

Darkening Effect on AZ31B Magnesium Alloy Surface Induced by Nanosecond Pulse Nd:YAG Laser

Y.C. Guan [1a b], W. Zhou [a b], H.Y. Zheng [b], Z.L. Li [b]

[a] *School of Mechanical and Aerospace Engineering, Nanyang Technological University, 50 Nanyang Avenue, Singapore 639798*

[b] *Singapore Institute of Manufacturing Technology, 71 Nanyang Drive, Singapore 638075*

Abstract

Permanent darkening effect was achieved on surface of AZ31B Mg alloy irradiated with nanosecond pulse Nd:YAG laser. Experiments were carried out to characterize morphological evolution and chemical composition of the irradiated areas by optical reflection spectrometer, Talysurf surface profiler, SEM, EDS, and XPS. The darkening effect was found to be occurred at the surface under high laser energy. Optical spectra showed that the induced darkening surface was uniform over the spectral range from 200 nm to 1100 nm. SEM and surface profiler showed that surface morphology of darkening areas consisted of large number of micron scale cauliflower-like clusters and protruding particles. EDS and XPS showed that compared to non-irradiated area, oxygen content at the darkening areas increased significantly. On the basis of above results, it was proposed a mechanism that involved trapping of light in the surface morphology and chemistry variation of irradiated areas to explain the laser-induced darkening effect on AZ31B Mg alloy.

Keywords: Darkening; Nanosecond Pulse Laser; Magnesium Alloy; Clusters; Oxidation.

1. Introduction

During the last decade, laser-induced darkening on materials surface has been widely studied due to its potential applications in many fields [1-6]. Malhotra *et al.*[1] reported laser-induced darkening in semiconductor-doped glasses with picosecond pulses, and they suggested that darkening was due to removal of the electrons from the microcrystallites to states in the amorphous glass host. Qian *et al.* [4, 5]

[1] Corresponding author: Tel: (65) 6793 8396; Fax: (65) 6791 6377; E-mail: guan0013@e.ntu.edu.sg

analyzed surface coloration on TiO_2 film irradiated with excimer laser, and explained that the darkening effect was due to trapping of light in the surface defects formed rather than anatase to rutile phase transformation as reported by others. Moreover, they found that surface morphology, such as the variation of surface roughness and defects, might play an important role in determining the color change at the surface of Ti following laser irradiation [6].

Mg alloys are important engineering materials, and they are widely used in the automobile, communication and aerospace fields due to low density and high specific strength [7-10]. In order to improve their poor surface-related properties, many experiments have been performed to demonstrate that laser surface treatment can be used to further extend the application of Mg alloy [11-15]. Here we present our work on darkening surface of AZ31B Mg alloy induced by nanosecond pulse Nd:YAG laser irradiation. The current study attempts to characterize surface morphology and chemistry of irradiated areas, with the aim of furthering the understanding of processes that lead to laser-induced darkening effect.

2. Experimental Procedures

The material studied was wrought AZ31B Mg alloy with the following chemical composition (wt. %): Al 2.89, Zn 0.87, Mn 0.39, Si 0.015, Cu 0.001, Ni 0.0005 and Mg balance. The specimens of dimensions 20 mm by 30 mm by 3 mm were ground with progressively finer SiC paper (180, 400, 800, 1200, 2400 and 4000 grit), cleaned with alcohol, and then irradiated with laser at atmospheric pressure and room temperature in air.

The nanosecond pulse Nd:YAG laser (with wavelength of 1064 nm and pulse duration 38 ns) was used by the following parameters: scanning speed 10 mm/s and frequency 6000 Hz. The laser was operated using a square beam spot of 1.2 mm side length, and the irradiated area was single track line in the surface with the length of 10 mm. Moreover, the values of laser average power were varied from 40 W to 110 W for line No. 1 to No. 5, as shown in Fig. 1. The average irradiation time was nearly 1 s for each area.

After laser irradiation, optical reflection of irradiated area at the specimen surface was measured using Ocean optics DT-Mini-2 system. All specimens were exposed to white light source, and reflected light from the surface was guided to HR4000 High-Resolution spectrometer to be analyzed by SpectraSuite

software. Each reflection measuring test was repeated three times. Before each test, the environment factor, such as fluorescent light and natural light, was excluded as reference. Microstructural features were investigated using a JEOL 5600 LV SEM, equipped with an EDS. The EDS measurements provided information on the chemical composition. Moreover, surface chemistry was studied using XPS with Kratos-Axis spectrometer. The spectra were calibrated using C 1 s peak position at 284.6 eV. Furthermore, surface topography of the irradiated areas was carried out using a Taylor Hobson Precision Talysurf profiler.

3. Results

Fig. 1 displays the darkening effect at AZ31B Mg alloy surface following nanosecond pulse Nd:YAG laser irradiation. It can be found that the irradiated areas at high laser power were very black from naked eyes, as indicated as No. 3, No. 4 and No. 5 in the figure.

Fig. 2 shows the optical reflection measurement of AZ31B Mg alloy surface before and after laser irradiation. When laser power was low, reflection pattern of irradiated areas No. 1 and No. 2 was similar to that of non-irradiated area, but reflection intensity decreased linearly with the increasing laser power. When laser power was high, the reflection pattern of irradiated areas No. 3, No. 4 and No. 5 experienced flattened reflectance spectra, and the reflection intensity dropped significantly. Moreover, the darkening areas were quite uniform over the spectral range from 200 nm to 1100 nm, and the average reflection intensity was nearly 0.13% of non-irradiated area in the visible light wavelength range from 390 nm to750 nm.

Morphological evolution of AZ31B Mg alloy surface after laser irradiation was investigated using SEM, as shown in Fig. 3. At low laser power, breakdown took place along fine scratch at the polished surface, and the irradiated areas were enlarged with laser power. Micro-cracks were also observed at the irradiated areas, as shown in Fig. 3(a), and Fig. 3(b). When laser power increased to 70 W and above, a large number of micron size cauliflower-like clusters together with some protruding particles were observed at the irradiated areas, as shown in Fig. 3(c)-(e). High magnification in Fig. 3(c)-(e) shows that the size of cauliflower-like clusters increased with laser power, and the protruding particles with less compact were above the clusters. Furthermore, it is interesting to note that the density of protruding

particles located in the center region of irradiated areas decreased with laser power significantly, but the density of protruding particles located at the boundary region did not change too much.

Surface topography of the darkening areas was further investigated using Talysurf surface profiler. The typical cauliflower-like clusters and large particles were found to be protruding above the substrate nearly 1.03 μm and 4.67 μm, respectively. Fig. 4 shows surface roughness Ra of AZ31B Mg alloy before and after laser irradiation. When laser power increased from 40 W to 70 W, Ra increased from 0.11 μm to 2.69 μm correspondingly. The reason for the maximum Ra value at 70 W was attributed to the cauliflower-like clusters and protruding particles at the irradiated area, as shown in Fig. 3(c). When laser power further increased to 110 W, Ra dropped linearly to 0.96 μm, and the reason was related to less protruding particles at the irradiated area, as shown in Fig. 3(c)-(e). Furthermore, the size distribution of clusters and particles located in the center region of irradiated areas was also studied, as shown in Fig. 5. The size of protrude particles decreased from 16 μm to 9 μm when laser power increased from 70 W to 110 W. This is in agreement with SEM results in Fig. 3.

Surface chemistry of laser-induced darkening AZ31B Mg alloy was analyzed using XPS and EDS. Fig. 6 shows the O 1s spectra at AZ31B Mg alloy surface. The binding energy peak at 531.5 eV was the peak of O 1s at non-irradiated surface, and the binding energy peak at 530.5 eV was the peak of O 1s at irradiated areas. The peak position change was likely due to the effect of $Mg(OH)_2$ and $MgCO_3$ [16, 17]. Before laser irradiation, $Mg(OH)_2$ and $MgCO_3$ existed at the polished surface of AZ31B Mg alloy due to atmospheric exposure [16]. After laser irradiation, $Mg(OH)_2$ and $MgCO_3$ disappeared gradually at the surface as a result of laser ablation, and the final peak position was attributed to MgO at the darkening area. Moreover, based on the quantitative analysis of EDS, both cauliflower-like clusters and protruding particles at the darkening area were identified as MgO, as shown in Fig. 7. Furthermore, average oxygen content at the irradiated areas increased from 5 wt% to 37 wt% with laser power, and such value was much higher than the average value of 4 wt% at the non-irradiated area.

4. Discussions

Short-pulse (several nanoseconds or shorter) laser irradiation of material surface initiates a complex sequence of events which occur both during and after the laser pulse, and the processes occurring between melted volume and plasma can lead to important chemical and physical modifications of surface properties [18-20].

Numerous research studies have been reported to demonstrate that the interaction of short laser pulse with target material leads to the formation of clusters and particles at the surface [21-24]. According to the findings of nanocluster synthesis by Itina *et al.* [21], the major advantage of short laser pulses for cluster synthesis was the presence of laser-ejected small species during laser material processing. In this study, when AZ31B Mg alloy was irradiated by nanosecond pulse laser, oxidation took place between the laser-ejected Mg alloy species in the ultrafast ablation plume and nearby oxygen in air, thereby leading to oxides formation [25]. Subsequently, the oxides deposited to the irradiated surface during rapid cooling condensation and plume collapse process [6, 8, 25].

However, it should be noted that the total laser irradiation time in this work was nearly 1 second as mentioned in the experimental procedure. According to Qian *et al.* [4, 5], the material redeposition would not be sufficient during the ultrafast laser process, and it was suggested that the effect of surface tension became another important contributor to the protrusion of irradiated surface. When laser power was high, hydrodynamic development at the irradiated areas occurred in addition to vaporization due to high thermal conductivity of Mg alloys [26, 27]. Hydrodynamic ablation resulted in the removal of material in the form of droplets, therefore isolated melt was formed, finally leading to the cauliflower-like clusters at the irradiated areas, as shown in Fig. 3. In addition, Luk' yanchuk *et al.* [28] reported that a decrease of laser fluence could induce a decrease of the aggregate size, thus leading to nucleation and development of particles above the clusters. Meanwhile, the shape of particles would become less compact due to greater volumetric heating upon successively repetitive pulse irradiation [24, 28]. Thereby, more large protruding particles were found at the irradiated areas where laser energy was low, as shown in Fig. 3 and Fig. 5. Moreover, both clusters and particles can trap light at the rough surface due to their morphology and topography based on the previous study [4-6, 25], and such effect will reduce the reflectance and cause the darkening effect, as shown in Fig. 1.

Therefore, it was suggested that the surface morphology played the dominate role in determining the laser-induced darkening effect on AZ31B Mg alloy surface after nanosecond pulse laser irradiation. In addition, the chemistry variation of irradiated areas due to oxidation also contributed to the darkening surface [5, 29, 30].

5. **Conclusions**

Laser-induced darkening surface was obtained on AZ31B Mg alloy following nanosecond pulse Nd:YAG laser irradiation in the presence of air. Color of the irradiated areas was uniform dark at high laser power. Surface morphology of darkening areas contained of cauliflower-like clusters and protruding particles. The formation of clusters and particles was mainly due to hydrodynamic ablation during laser irradiation, and less compact but large particles were formed above the clusters due to greater volumetric heating when laser energy was low. It was proposed that the darkening effect was mainly attributed to light trapping in the rough surface of irradiated areas, and surface chemistry variation played a second role in determining the color change.

References

1. J. Malhotra, D.J. Hagan, B.G. Potter, J. Opt. Soc. Am. B-Opt. Phys. 8(1991):1531-1536;
2. V. Bichevin, H KaÈaÈmbre, Phys. Stat. Sol. B 186(1994):57-70;
3. Y. Zhao, Z.C. Feng, Y. Liang, H.W. Sheng, Appl. Phys. Lett. 71(1997):2227-2229;
4. H.X. Qian, W. Zhou, H.Y. Zheng, Surf. Rev. Lett. 15(2008):473-479;
5. H.Y. Zheng, H.X. Qian, W. Zhou, Appl. Surf. Sci. 254(2008):2174-2178;
6. H.X. Qian, W. Zhou, H.Y. Zheng, Surf. Rev. Lett. 15(2008):675-679;
7. Y.J. Huang, B.H. Hu, I. Pinwill, W. Zhou, D.M.R. Taplin, Mater. Manuf. Proc. 15 (2000):97-105;
8. K. Matsubara, Y. Miyahara, Z Horitaa, T.G. Langdon, Acta Mater. 51(2003):3073-3084;
9. Y.C. Guan, W. Zhou, Mater. Lett. 62 (2008):4494-4496;
10. R. Ambat, N.N. Aung, W. Zhou, Corr. Sci. 42(2000):1433-1455;

11. J.E. Gray, B. Luan, J. Alloys. Compd. 336(2002):88-113;
12. Y.C. Guan, W. Zhou, H.Y. Zheng, J. Appl. Electrochem. 39(2009):1457-1464;
13. L.F. Cai, C.K. Mark, W. Zhou, Sur. Rev. Lett. 16 (2009):215-221;
14. Y.C. Guan, W. Zhou, H.Y. Zheng, Z.L. Li, Appl. Phys. A, 101 (2010):339-344;
15. Y.C. Guan, W. Zhou, Z.L. Li, H.Y. Zheng, Appl. Surf. Sci., 255 (2009):8235-8238;
16. S. Ardizzone, C.L. Bianchi, M. Fadoni, B. Vercelli, Appl. Surf. Sci. 119(1997):253-259;
17. V. Fournier, P. Marcus, I. Olefjor, Surf. Interface. Anal. 34 (2002):494-497;
18. H.G. Rubahn, Laser Applications in Surface Science and Technology. John Wiley & Sons, 1999;
19. W.M. Steen, Laser Material Processing. Springer, London, UK, 2003;
20. M.S. Tillack, D.W. Blair, S.S. Harilal, Nanotechnol. 15(2004):390-403 ;
21. T.E. Itina, K. Gouriet, L.V. Zhigilei, S. Noël, J. Hermann, M. Sentis, Appl. Surf. Sci. 253(2007):7656-7661;
22. D.B. Geohegan, A.A. Puretzky, G. Dusher, S.J. Pennycook, Appl. Phys. Lett. 72(1998):2987-2989;
23. W. Marine, L. Patrone, B. Luk'yanchuk, M. Sentis, Appl. Surf. Sci. 154(2000):345-352 ;
24. A. Pereira, A. Cros, P. Delaporte, S. Georgiou, A. Manousaki, W. Marine, M. Sentis, Appl. Phys. A 79 (2004):1433-1437;
25. H.X. Qian, W. Zhou, H.Y. Zheng, G.C. Lim, Surf. Sci. 595(2005):49-55;
26. M.M. Avedesian, H. Baker, Magnesium and magnesium alloys. ASM International, Handbook Committee, 1999;
27. X. Zhang, S.S. Chu, J.R. Ho, C.P. Grigorpoulos, Appl. Phys. A 64(1997):545-552;
28. B.S. Luk'yanchuk, W. Marine, S.I. Anisimov, Laser Phys. 8(1998):291-302;
29. Y.F. Lu, H. Qiu, J. Appl. Phys. 88(2000):1082-1087;
30. Z.L. Li, H.Y. Zheng, K.M. Teh, Y.C. Liu, G.C. Lim, H.L. Seng, N.L. Yakovlev, Appl. Surf. Sci. 256(2009):1582-1588.

Figure captions

Fig. 1 Photo showing colors of the irradiated areas with increasing laser power on AZ31B Mg alloy surface induced by nanosecond pulse Nd:YAG laser in air, where **1** represented 40 W, **2** represented 60 W, **3** represented 70 W, **4** represented 90 W, and **5** represented 110 W.

Fig. 2 Optical reflection measurement of non-irradiated area and irradiated areas at AZ31B Mg alloy surface in Fig. 1.

Fig. 3 SEM images showing morphological evolution of AZ31B Mg alloy surface after irradiation with progressive laser power: (a) 40 W; (b) 60 W; (c) 70 W; (d) 90 W; (e) 110 W. High magnification images from the areas were also shown.

Fig. 4 Surface roughness Ra of AZ31B Mg alloy before and after laser irradiation

Fig. 5 Size distribution of clusters and particles at the irradiated areas of the AZ31B Mg alloy surface: (a) 70 W, (b) 90 W and (c) 110 W.

Fig. 6 XPS spectra showing O 1s peak at non-irradiated area and irradiated areas at AZ31B Mg alloy surface in Fig. 1.

Fig. 7 Morphology and chemical composition of typical cauliflower-like clusters and protruding particle at the irradiated area of AZ31B Mg alloy with 70 W: (a) SEM image; (b)-(c) Chemical composition for the cluster (A) and particle (B).

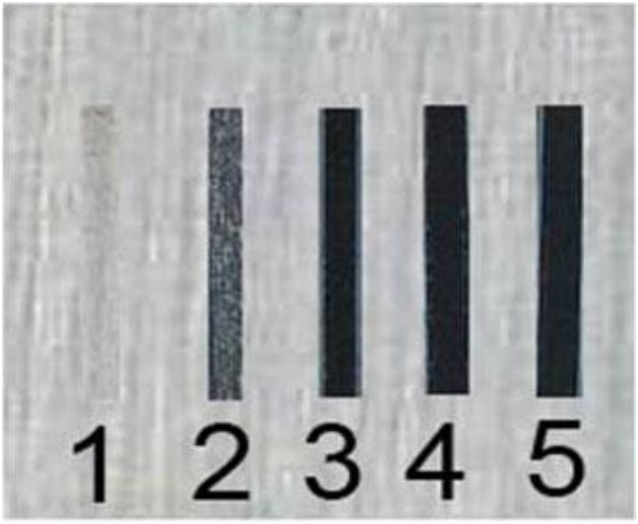

Fig. 1

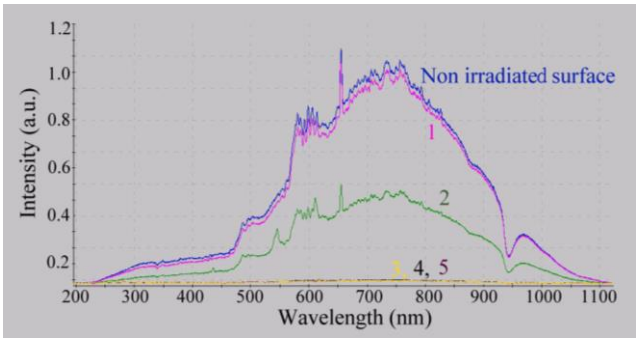
Intensity (a.u.)
Wavelength (nm)
Non irradiated surface
1
2
3, 4, 5

Fig. 2

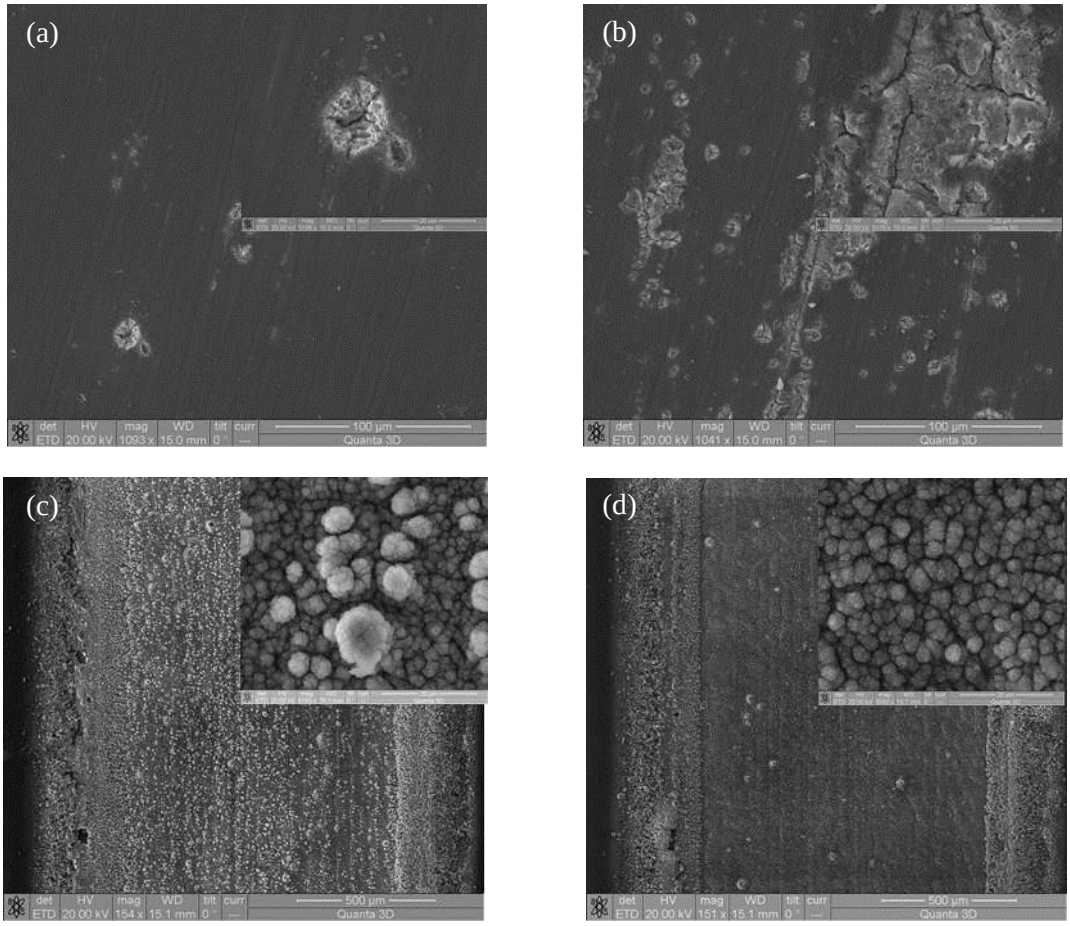
(a)
(b)
(c)
(d)

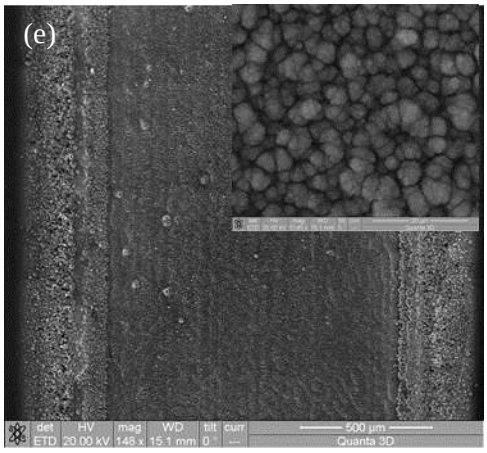

Fig. 3

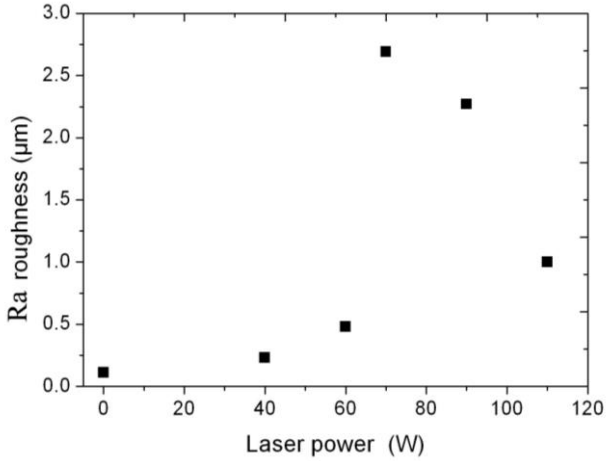

Fig. 4

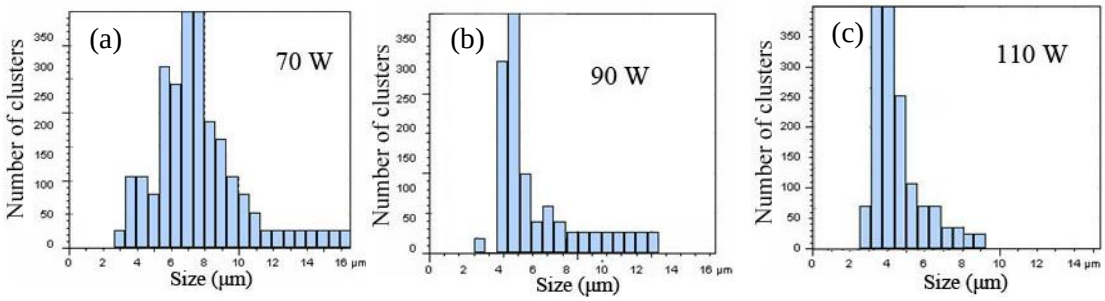

Fig. 5

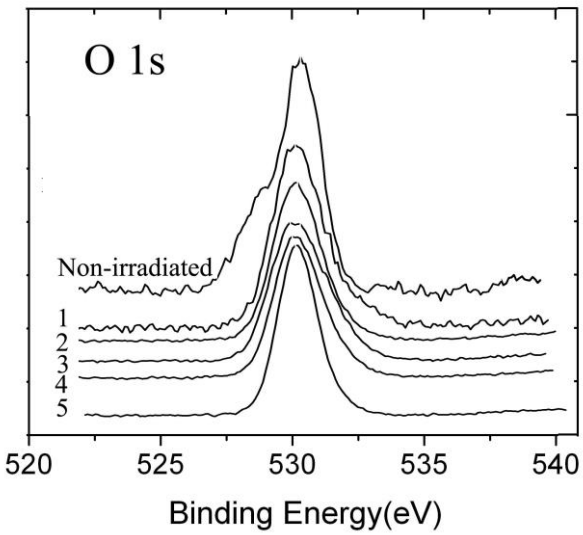
O 1s
Non-irradiated
1
2
3
4
5
520
525
530
535
540
Binding Energy(eV)

Fig. 6

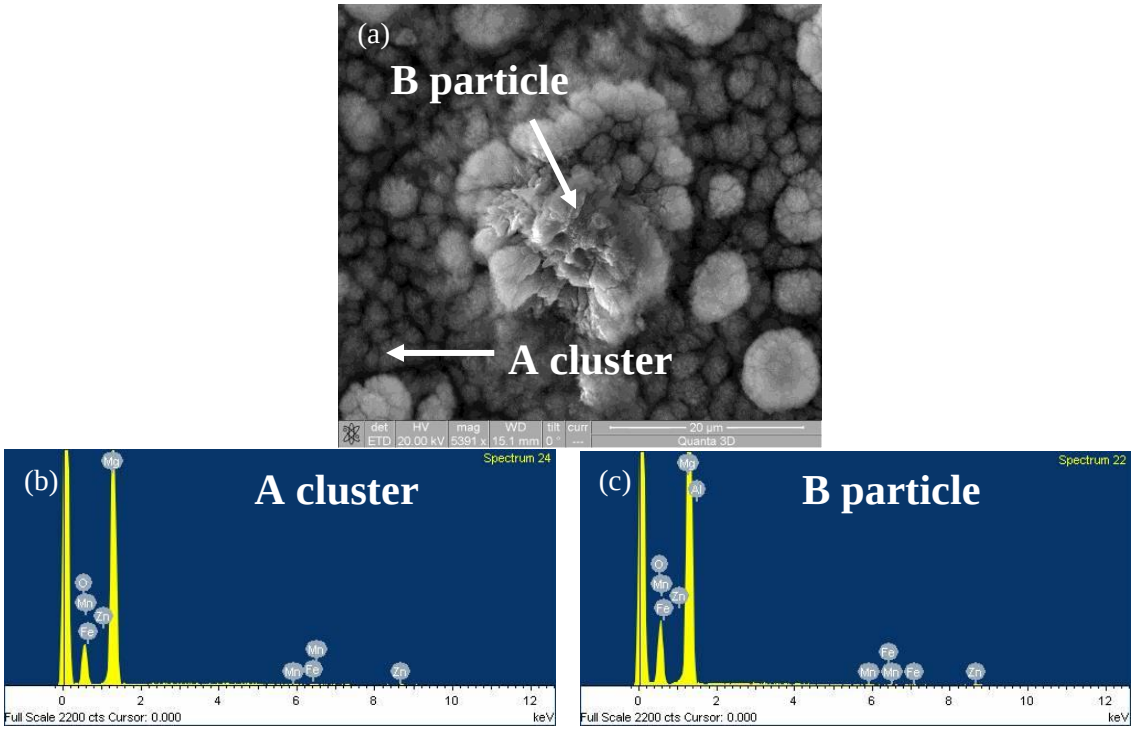
(a)
B particle
A cluster
(b)
A cluster
Spectrum 24
Full Scale 2200 cts Cursor: 0.000
keV
(c)
B particle
Spectrum 22
Full Scale 2200 cts Cursor: 0.000
keV

Fig. 7